Carbon Dots

DOI: 10.1002/anie.201411004

Tunable Photoluminescence Across the Entire Visible Spectrum from Carbon Dots Excited by White Light**

Shengliang Hu, Adrian Trinchi,* Paul Atkin, and Ivan Cole*

Abstract: *Although reports have shown shifts in carbon dot emission wavelengths resulting from varying the excitation wavelength, this excitation-dependent emission does not constitute true tuning, as the shifted peaks have much weaker intensity than their dominant emission, and this is often undesired in real world applications. We report for the first time the synthesis and photoluminescence properties of carbon dots whose peak fluorescence emission wavelengths are tunable across the entire visible spectrum by simple adjustment of the reagents and synthesis conditions, and these carbon dots are excited by white light. Detailed material characterization has revealed that this tunable emission results from changes in the carbon dots' chemical composition, dictated by dehydrogenation reactions occurring during carbonization. These significantly alter the nucleation and growth process, resulting in dots with either more oxygen-containing or nitrogen-containing groups that ultimately determine their photoluminescence properties, which is in stark contrast to previous observations of carbon dot excitation-dependent fluorescence. This new ability to synthesize broadband excitable carbon dots with tunable peak emissions opens up many new possibilities, particularly in multimodal sensing, in which multiple analytes and processes could be monitored simultaneously by associating a particular carbon dot emission wavelength to a specific chemical process without the need for tuning the excitation source.*

Fluorescent carbon dots (CDs) exhibit great potential in bioimaging and biosensing due to their biocompatible, nontoxic, excellent chemical and photostability as well as superior optical properties.[1] They usually consist of a graphene-based core and carbonaceous surface.[1e,2] However, unlike pristine graphene, which does not possess an electronic bandgap in the visible light region,[1e,2b,c,3] bandgap formation, and hence light emission, in CDs is attributed to structural defects induced by finite size and element doping (e.g., O, N).[1e,2a,4] This results in the nonstoichiometric nature of CDs and thus tailor-made control of their optical properties is extremely challenging.[1d,4c]

Obtaining fluorescence emission across the entire visible spectrum has been recognized as a key requirement for successfully implementing carbon dots in nearly all practical applications.[1f,2e,4c,5] Although many reports have presented excitation-dependent fluorescence emission, the relative wavelength shifts tend not to cover the entire visible spectrum,[2c,4c–e,5a,c,6] typically being in the order of 100 to 150 nm and accompanied by a significant decrease in fluorescence emission intensity.[2c,4c–e,5a,c,6] Such optical shifts cannot be truly labeled "tunable". What is truly sought is a means for varying the CDs chemical and physical properties to achieve a shift in the emission wavelength, and which can be excited by broadband light (similar to semiconductor quantum dots) without compromising the peak emission intensity. Whilst highly desired, achieving this has remained elusive thus far. Synthesizing CDs capable of meeting these criteria has proven challenging and, unlike with semiconductor quantum dots, this cannot be achieved by simply changing the particle size alone.[1e,4c–e,6b,e] Although various synthesis techniques have been developed in recent years,[1d,e,2b,4a] they have not been shown to tune photoluminescence (PL) peak emission wavelengths of CDs across the entire visible light spectrum by one single method.

Herein we report for the first time an approach to shift PL peaks of CDs to cover the entire visible spectrum (400–710 nm) by controlling the dehydration reaction occurring during synthesis. This is achieved by tuning the reagents. The obtained CDs exhibit five colors spanning from blue to red when excited by white light, and thus are extremely promising for many applications, e.g., biolabeling, bioimaging, and the sensitive determination of targets due to large penetration depths, low harm, and background associated with using white light excitation rather than UV.[1b,7]

CDs were prepared by modifying a previously reported method[8] and our synthetic strategy is shown in Figure 1 (further details can be found in the Supporting Information, SI). Citric acid (CA) or ethylene glycol (EG) was mixed with ethylenediamine endcapped polyethylenimine ($M_n = 600$, PEI-EC, purchased from Sigma–Aldrich) in MilliQ water. The appropriate amounts of $NaBH_4$ (98%, purchased from Sigma-Aldrich) or H_3PO_4 (99%, purchased from Sigma-Aldrich) were added in the mixture based on the experimen-

[*] Prof. S. Hu
School of Material Science and Engineering
North University of China
Taiyuan 030051 (P. R. China)
E-mail: hsliang@yeah.net
Dr. A. Trinchi, P. Atkin, Prof. I. Cole
CSIRO Materials Science and Engineering
I Private Bag 33, Clayton 3169 (Australia)
E-mail: Adrian.Trinchi@csiro.au

[**] We thank the National Natural Science Foundation of China (grant numbers 51272301 and 51172214), the China Postdoctoral Science Foundation (grant numbers 2012M510788 and 2013T60269), the Shanxi Province Science Foundation for Youths (2014021008), 131 Talent Plan of Higher Learning Institutions of Shanxi, and the China Scholarship Council Fund for financial support. We also thank the CSIRO Sensor and Sensor Networks Transformational Capability Platform.

Supporting information for this article is available on the WWW under http://dx.doi.org/10.1002/anie.201411004.

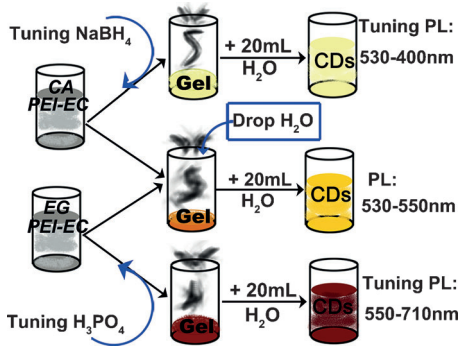

Figure 1. Synthesis of CDs with different emission colors.

tal design to yield either blue or red shifts in the peak PL emission, and the mixtures were heated to 180 °C with a heating mantle. When the gel was formed, 2 mL of MilliQ water was added to prevent it from scorching and heating was continued. This procedure was repeated five times until finally CDs with tunable PL peaks were obtained and the solution adjusted to 20 mL with MilliQ water. The concentrations of the obtained CDs are 0.32–0.37 g L^{-1}. For each synthesized type of carbon dot there was an optimal emission peak, though in some cases (at longer wavelengths) a shift in emission with varying excitation was observed (Figure 2 a–f).

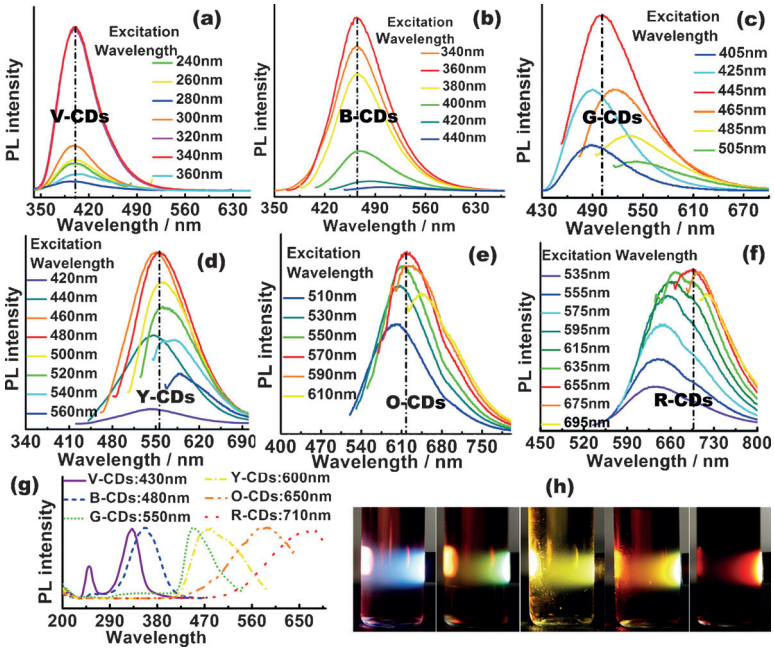

Figure 2. a–f) PL spectra of V-, B-, G-, Y-, O-, and R-CDs, showing different strongest emission peaks. g) PLE spectra of the six samples; h) emission photos of different CDs excited by white light.

In each case, however, only one optimal excitation wavelength, commonly corresponding to the PL excitation (PLE) peak, was found to excite the strongest emission (Figure 2 g). This strongest emission peak reflects the CDs most dominant energy gap, and for each sample it depends on the synthesis reagents and reaction conditions. From Figure 2 a–f, the strongest PL peaks of the prepared six samples are around 400, 460, 500, 540, 610, and 710 nm, and are named V-, B-, G-, Y-, O-, and R-CDs, respectively. According to Figure 2 g, PLE peaks also change with the samples and exhibit a shift to the red light region. Five different colors (Figure 2 h) are obtained upon irradiation of B-, G-, Y-, O-, and R-CDs with white light.

Although changing the reaction temperature did cause a shift in the peak PL emission (increased temperature causing red shifts), these shifts were small and limited to only a very narrow range, demonstrating that reaction temperature did not play a vital role in tuning. Interestingly, the CDs whose strongest PL peaks occurred at 530–550 nm could be obtained by directly pyrolyzing either CA or EG in the presence of PEI-EC; however, despite having a similar PL emission range, there were differences in their PL and PLE spectra (see Figure S2a). Under the same synthesis conditions, the EG-based CDs show broader PL spectra and more PLE peaks than the CA-based CDs, possibly arising from the changing molecular types as carbon sources.

The PL peak emission was tuned by adding either a dehydrating agent (H_3PO_4) or a reducing agent ($NaBH_4$) to the reaction system (CA + BPEI-EC or EG + BPEI-EC), see Figure S2b and c.[1d,4b] Adding H_3PO_4 to EG-based CDs caused the strongest PL peak to redshift, and the degree of redshifting was proportional to the amount of added H_3PO_4. However, adding H_3PO_4 to the CA-based CDs did not change their PL properties(Figure S2b). Conversely, adding $NaBH_4$ to CA and EG reaction systems resulted in a blueshift of the CDs strongest PL peak (Figure S2c). Here the degree of blueshifting increases with the amount of $NaBH_4$ added to the CA solution only, whereas further $NaBH_4$ additions to EG had little effect. Although the PEI-EC itself cannot shift the peak PL position, it can influence the PL intensities of CDs prepared from CA, whilst having little effect on the PL intensities of those prepared from EG (Figure S2d). From these results it is clear that the strongest PL can be tailored by controlling the amount of H_3PO_4 and $NaBH_4$ added to the CA and EG starting solutions, respectively. In this way it was possible to shift the CDs peak PL emission across the entire visible spectrum (Figure 2 a–f), that is, adding $NaBH_4$ to CA solutions tunes the emission from violet to yellow, and adding H_3PO_4 to EG solutions shifts the emission from yellow to red. Based on the synthetic mechanism of CDs with organic molecules, the addition of H_3PO_4 and $NaBH_4$ could change the dehydrogenation reactions occurring during the carbonization of CA and EG (see SI), thus resulting in different optical properties of CDs.

The obtained CDs' size distributions were measured by dynamic light scattering (DLS). The particle diameters in B-, Y-, and R-CDs range from 1–12 nm, 2–8 nm, and 5–11 nm, respectively (Figure 3 a). These results were further confirmed by TEM (Figure 3 b and c). According to Figure 2 b,d and f, B-CDs with a broader size distribution show less excitation-wavelength-dependent PL behavior than

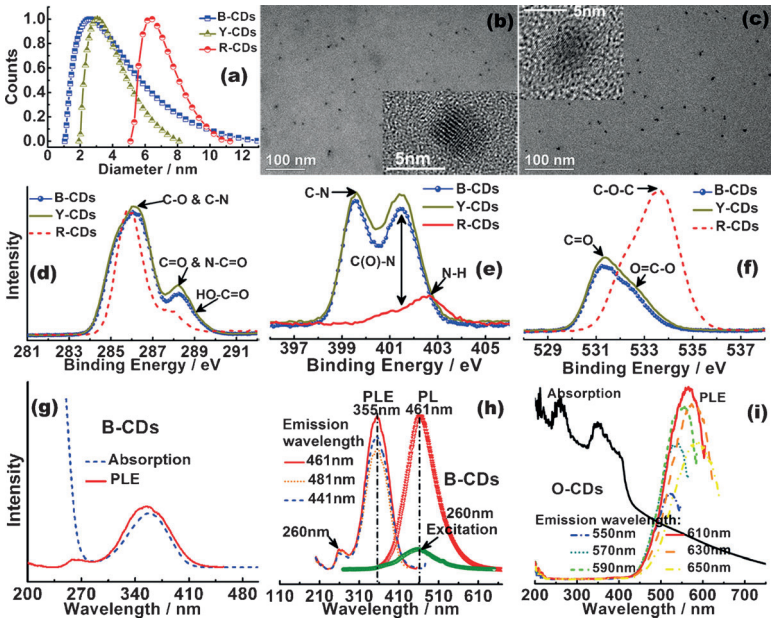

Figure 3. a) DLS results of B-, Y-, and R-CDs; b) and c) TEM and HRTEM images of B- and R-CDs; d–f) C1s, N1s, and O1s spectra of B-, Y-, and R-CDs, respectively; g) PLE and absorption spectra of B-CDs; h) PL of B-CDs excited at 355 and 260 nm and PLE spectra collected at different emission wavelengths; i) Absorption of O-CDs and their PLE spectra collected at different emission wavelengths.

Y- or R-CDs with a narrower size distribution. CDs with much wider size ranges were obtained by adding H_3PO_4 to a CA solution (Figure S3a), despite exhibiting the same PL peak with Y-CDs (Figures 2d and S1b) and therefore the particle size alone cannot be the limiting factor for tuning CDs PL properties. This observation has also been made recently.[9] High-resolution TEM images suggest that CDs' have complicated structures. Carbon nanocrystals are found in both B- and R-CDs (inset of Figure 3b and c), whereas many amorphous structures are also observed. Although structural defects have been proposed to create bandgaps in CDs,[1e] an explanation of the relationship between structural defects and bandgaps remains the subject of much debate. Many efforts have indicated that an alternative way to realize energy gap changes in CDs is tailoring their surface-related defective sites through surface compositions.[1f,4a,e,5,6e,10]

The CDs compositions were determined by X-ray photoelectron spectroscopy (XPS), showing the CDs oxygen content increases with the redshift of the strongest PL peaks. For example, 22.25%, 24.34%, and 48.34% O atoms are contained in B-, Y-, and R-CDs, respectively, and their corresponding N contents are 14.49%, 14.395%, and 2.29%, respectively. The C 1s, N 1s, and O 1s signals of B-, Y-, and R-CDs present clear differences in the N- and O-related bonds (Figure 3d–f). C–O bonding can be observed in all samples, whereas the amount of C–O–C bonds in the R-CDs is greater than those in both B- and Y-CDs. Compared to the B- and Y-CDs, the R-CDs have much less C=O and C–N bonds. These results were confirmed by ^{13}C NMR spectra (Figure S4), in which the stronger C–O–C and weaker C=O signals were observed in R-CDs than in the B- and Y-CDs. Moreover, the CDs prepared by adding the same amount of H_3PO_4 with O-CDs to CA solution showed no obvious changes in their PL features except for a narrower full width at half maximum (Figures 2a and S2b), though their composition and C 1s, N 1s, and O 1s spectra show some differences in contrast to CA-based Y-CDs (Figure S3b–d). Accordingly, the energy gap in the CDs not only relies on the total N and O content, but on the relative amount of different types of carbon bonding with N and O, which is also supported by theoretical calculations and experimental results reported previously.[2a,11] Such appropriate conditions in CDs could be attributed to the changes of molecular types as carbon sources and even the addition of H_3PO_4 and $NaBH_4$ in reaction system.

All samples show a shoulder absorption peak at 300–400 nm, attributed to n–π* transitions of C=O[12] (Figure S5). In particular, this absorption peak of B-CDs (or V-CDs) almost overlaps with their PLE peak (Figure 3g). As shown in Figure 3h the B-CDs PLE peak positions remain unchanged (except for their intensities) for each emission wavelength recorded. Even when higher-energy wavelengths were employed to excite fluorescence, such as 260 nm, which is attributed to π–π* transitions of C=C,[1f,5] the same emission wavelength was observed as that from 355 nm excitation. Therefore, the CDs emission could be derived from the radiative recombination of the excited electrons from the n–π* transitions of C=O.[1f,12] For the G-, Y-, O-, and R-CDs, an absorption tail is observed that extends to the visible region (Figures 3i and S5), and their PLE peaks cannot overlap with the shoulder in their absorption peaks. Furthermore, their PLE peaks change with the collected emission wavelengths (Figure 3i). Fluorescence lifetimes are on the ns timescale, revealing the singlet state nature of their emission (Figure S6). CDs exhibit different fluorescence lifetimes and they become longer with the increase of the amount of C–O bonds (e.g., O-CDs have longer lifetime than B- and Y-CDs), confirming the existence of different types of electronically excited states. According to theoretical predications reported by Chien et al.,[11] a series of new absorption bandgaps is gradually created as the O content increases. Accordingly, there should be a series of energy transitions between bandgaps and a pathway to radiative recombination in the most popular manner, resulting in broad PL spectra with only one dominant peak. Because more electronic structures cause more possible recombination, including nonradiative recombination, quantum yields of CDs decrease as their PL emission becomes red-shifted (Figure S1).

Based on first-principle calculations of Yan et al.,[2a] the C–O–C and C–OH groups on sp^2-hybridized carbons can induce significant local distortion and then create various energy gaps. Such new energy gaps could be located in the band tail of the π–π* gap. Due to the formation of C=O in CDs, the n–π* transitions become predominant. Thus, V- and B-CDs exhibit excitation-wavelength-independent emission and their PLE peak and shoulder absorption peak are overlapped. With the increase of C–OH and C–O–C

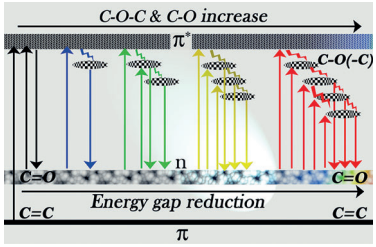

Figure 4. Illustration of the tunable PL emission from CDs containing different O-related surface groups.

groups in CDs, a large number of epoxide (or hydroxy)-related localized electronic states are expected to form below the π* state,[11] creating numerous new energy levels between n–π* gaps (schematized in Figure 4). Consequently, many kinds of the radiative recombination could occur,[12] causing a wide range of excitation energies and excitation-wavelength-dependent PL (Figure 2 c–f). In fact, from Figure 2 f, two PL peaks are observed in R-CDs due to more recombination possibilities.[1f,12] PEI-EC with NH_2 groups could act as surface passivation, facilitating more effective radiative recombination of surface-confined electrons and holes, though some believed that C–N bonds can alter electronic structures.[1,4,8] However, CDs or graphene oxide without amino groups can still emit fluorescence.[11,12] Hence, the O-containing groups in CDs could play a key role in the creation of energy gaps and result in tunable PL.

This new ability to tune the fluorescence emission peak across the entire visible spectrum is not only beneficial in terms of the novel chemistry and understanding the reagents' role in the CD structure and PL properties, but also enables new research opportunities in the application of CDs. One key application area for multicolored emission CDs is multimodal sensing,[13] particularly in biology. Owing to the biocompatibility of CDs, functionalization with, or attachment to, biological species could allow direct observation of multiple biological reactions and processes simultaneously by assigning a different colored CD to a different process. Irradiating the entire system with broadband white light could yield a sensory color map based on the acquired fluorescence images, in which the CDs' color distribution or intensity could be used to analyze parameters such as reaction rate, kinetics, or bonding specificity. Another application area is tracers for inline downstream processing, in which different colors could be coupled to analyte species of interest, say blue for pH, green for a specific molecule, yellow with dissolved oxygen, etc. Clearly the ability to tailor light emission means color can be associated to specific chemistries in chemically sensitive environments.

In conclusion, an approach to tailor the energy gap and hence the fluorescence emission wavelength in CDs that are excited by white light has been developed. This resulted in the peak emission wavelength being tunable across the entire visible spectrum, from blue all the way through to deep red, by a simple adjustment of the reagents and synthesis conditions. We found that this was largely a result of the dehydrogenation reactions occurring during carbonization, which significantly alter the nucleation and growth process, resulting in dots with either more oxygen-containing or nitrogen-containing groups. Accordingly, the energy gap in the CDs not only relies on the total level of N and O content but also on the relative amount of different types of carbon bonding with N and O, which is also supported by theoretical calculations and experimental results reported previously. Therefore, this work provides requirements for the successful implementation of carbon dots. We anticipate these carbon dots can be utilized in wide ranging applications such as illumination, electronic devices, and particularly in biosensing, opening the possibility for monitoring multiple analytes or species simultaneously without the need for tuning the excitation source.

Received: November 13, 2014
Published online: January 14, 2015

Keywords: carbon dots · doping · fluorescent nanoparticle · luminescence · surface groups

[1] a) Y.-P. Sun, B. Zhou, Y. Lin, W. Wang, K. A. S. Fernando, P. Pathak, M. J. Meziani, B. A. Harruff, X. Wang, H. Wang, P. G. Luo, H. Yang, M. E. Kose, B. Chen, L. M. Veca, S.-Y. Xie, *J. Am. Chem. Soc.* **2006**, *128*, 7756–7757; b) L. Cao, X. Wang, M. J. Meziani, F. Lu, H. Wang, P. G. Luo, Y. Lin, B. A. Harruff, L. M. Veca, D. Murray, S.-Y. Xie, Y.-P. Sun, *J. Am. Chem. Soc.* **2007**, *129*, 11318–11319; c) C. Liu, P. Zhang, X. Zhai, F. Tian, W. Li, J. Yang, Y. Liu, H. Wang, W. Wang, W. Liu, *Biomaterials* **2012**, *33*, 3604–3613; d) S. K. Bhunia, A. Saha, A. R. Maity, S. C. Ray, N. R. Jana, *Sci. Rep.* **2013**, *3*, 1473; e) L. Cao, M. J. Meziani, S. Sahu, Y.-P. Sun, *Acc. Chem. Res.* **2013**, *46*, 171–180; f) H. Nie, M. Li, Q. Li, S. Liang, Y. Tan, L. Sheng, W. Shi, S. X.-A. Zhang, *Chem. Mater.* **2014**, *26*, 3104–3112.

[2] a) J.-A. Yan, L. Xian, M. Y. Chou, *Phys. Rev. Lett.* **2009**, *103*, 086802; b) L.-s. Li, X. Yan, *J. Phys. Chem. Lett.* **2010**, *1*, 2572–2576; c) X. Yan, B. Li, X. Cui, Q. Wei, K. Tajima, L.-s. Li, *J. Phys. Chem. Lett.* **2011**, *2*, 1119–1124; d) X. Yan, B. Li, L.-s. Li, *Acc. Chem. Res.* **2013**, *46*, 2254–2262; e) L. Tang, R. Ji, X. Li, G. Bai, C. P. Liu, J. Hao, J. Lin, H. Jiang, K. S. Teng, Z. Yang, S. P. Lau, *ACS Nano* **2014**, *8*, 6312–6320.

[3] Z. Luo, P. M. Vora, E. J. Mele, A. T. C. Johnson, J. M. Kikkawa, *Appl. Phys. Lett.* **2009**, *94*, 0.

[4] a) Y. Li, Y. Zhao, H. Cheng, Y. Hu, G. Shi, L. Dai, L. Qu, *J. Am. Chem. Soc.* **2012**, *134*, 15–18; b) H. Zheng, Q. Wang, Y. Long, H. Zhang, X. Huang, R. Zhu, *Chem. Commun.* **2011**, *47*, 10650–10652; c) H. Tetsuka, R. Asahi, A. Nagoya, K. Okamoto, I. Tajima, R. Ohta, A. Okamoto, *Adv. Mater.* **2012**, *24*, 5333–5338; d) D. Sun, R. Ban, P.-H. Zhang, G.-H. Wu, J.-R. Zhang, J.-J. Zhu, *Carbon* **2013**, *64*, 424–434; e) X. Li, S. Zhang, S. A. Kulinich, Y. Liu, H. Zeng, *Sci. Rep.* **2014**, *4*, 4976.

[5] a) S. H. Jin, D. H. Kim, G. H. Jun, S. H. Hong, S. Jeon, *ACS Nano* **2013**, *7*, 1239–1245; b) S. Zhu, J. Zhang, S. Tang, C. Qiao, L. Wang, H. Wang, X. Liu, B. Li, Y. Li, W. Yu, X. Wang, H. Sun, B. Yang, *Adv. Funct. Mater.* **2012**, *22*, 4732–4740; c) S. Zhu, Q. Meng, L. Wang, J. Zhang, Y. Song, H. Jin, K. Zhang, H. Sun, H. Wang, B. Yang, *Angew. Chem. Int. Ed.* **2013**, *52*, 3953–3957; *Angew. Chem.* **2013**, *125*, 4045–4049.

[6] a) Z.-C. Yang, M. Wang, A. M. Yong, S. Y. Wong, X.-H. Zhang, H. Tan, A. Y. Chang, X. Li, J. Wang, *Chem. Commun.* **2011**, *47*, 11615–11617; b) Y.-Q. Zhang, D.-K. Ma, Y. Zhuang, X. Zhang, W. Chen, L.-L. Hong, Q.-X. Yan, K. Yu, S.-M. Huang, *J. Mater. Chem.* **2012**, *22*, 16714–16718; c) Y. Sun, S. Wang, C. Li, P. Luo, L. Tao, Y. Wei, G. Shi, *Phys. Chem. Chem. Phys.* **2013**, *15*, 9907–9913; d) J. Zhou, Y. Yang, C.-y. Zhang, *Chem. Commun.* **2013**,

49, 8605 – 8607; e) S. Yang, J. Sun, X. Li, W. Zhou, Z. Wang, P. He, G. Ding, X. Xie, Z. Kang, M. Jiang, *J. Mater. Chem. A* **2014**, *2*, 8660 – 8667.

[7] a) X. Ouyang, J. Liu, J. Li, R. Yang, *Chem. Commun.* **2012**, *48*, 88 – 90; b) S. Chen, X. Hai, C. Xia, X.-W. Chen, J.-H. Wang, *Chem. Eur. J.* **2013**, *19*, 15918 – 15923.

[8] a) Y. Dong, R. Wang, G. Li, C. Chen, Y. Chi, G. Chen, *Anal. Chem.* **2012**, *84*, 6220 – 6224; b) Y. Dong, R. Wang, H. Li, J. Shao, Y. Chi, X. Lin, G. Chen, *Carbon* **2012**, *50*, 2810 – 2815.

[9] G. S. Kumar, R. Roy, D. Sen, U. K. Ghorai, R. Thapa, N. Mazumder, S. Saha, K. K. Chattopadhyay, *Nanoscale* **2014**, *6*, 3384 – 3391.

[10] J. Peng, W. Gao, B. K. Gupta, Z. Liu, R. Romero-Aburto, L. H. Ge, L. Song, L. B. Alemany, X. B. Zhan, G. H. Gao, S. A. Vithayathil, B. A. Kaipparettu, A. A. Marti, T. Hayashi, J. J. Zhu, P. M. Ajayan, *Nano Lett.* **2012**, *12*, 844 – 849.

[11] C.-T. Chien, S.-S. Li, W.-J. Lai, Y.-C. Yeh, H.-A. Chen, I. S. Chen, L.-C. Chen, K.-H. Chen, T. Nemoto, S. Isoda, M. Chen, T. Fujita, G. Eda, H. Yamaguchi, M. Chhowalla, C.-W. Chen, *Angew. Chem. Int. Ed.* **2012**, *51*, 6662 – 6666; *Angew. Chem.* **2012**, *124*, 6766 – 6770.

[12] Z. X. Gan, S. J. Xiong, X. L. Wu, T. Xu, X. B. Zhu, X. Gan, J. H. Guo, J. C. Shen, L. T. Sun, P. K. Chu, *Adv. Opt. Mater.* **2013**, *1*, 926 – 932.

[13] O. Obst, A. Trinchi, S. G. Hardin, M. Chadwick, I. Cole, T. H. Muster, N. Hoschke, D. Ostry, D. Price, K. N. Pham, T. Wark, *Nano Commun. Networks* **2013**, *4*, 189 – 196.

